Photochemistry of $Fe(CO)_5$ Adsorbed on Single Crystal and Roughened Silver

Daren J. Burke, Tomas Vondrak, and Stephen R. Meech*

School of Chemical Sciences, University of East Anglia, Norwich NR4 7TJ, U.K.

Received: May 23, 2002; In Final Form: July 23, 2002

The photochemistry of $Fe(CO)_5$ adsorbed on silver at 89 K has been investigated by time-of-flight mass spectrometry, thermal desorption spectroscopy, and photon-induced desorption. These measurements were made as a function of coverage, decane spacer layer thickness, and surface roughness. Photodissociation yields CO in the gas phase. Wavelength dependent studies of the cross-section suggest an adsorbate-mediated mechanism. Time-of-flight data reveal both translationally hot and thermalized CO products, the latter being more prominent when the adsorbate is not directly adsorbed onto the silver surface. The photochemical cross-section is found to be larger for $Fe(CO)_5$ adsorbed directly onto silver than for adsorption onto decane or for multilayers. In contrast the photochemical yield is larger for multilayer coverage. It is proposed that this is in part due to the existence of dark reactions between the photoproduct and the reactant, which occur more readily in multilayers. The effect of extensive roughening of the surface is to enhance the photochemical cross-section by at most a factor of 2. This suggests that surface-plasmon-enhanced photochemistry is of only minor importance in this case.

1. Introduction

In this paper we report a comprehensive investigation of the photochemistry of $Fe(CO)_5$ adsorbed on silver. Photochemical dynamics are interrogated by means of time-of-flight (TOF) mass spectrometry. The photochemical mechanism and cross-section are investigated using thermal desorption (TD) spectroscopy and wavelength-resolved photon-induced desorption (PID) measurements, respectively. All measurements are made as a function of coverage, adsorbate−surface distance, and surface roughening. These data provide a more detailed picture of the photochemistry of adsorbed $Fe(CO)_5$, resolving some anomalies in the literature, and yielding further insight into the effect of surface morphology on adsorbate-mediated photochemistry.

The photodissociation of iron pentacarbonyl has an important place in the study of photochemical reactions on metal surfaces. It was among the first adsorbates for which photochemistry was unambiguously identified.[1] Previously it had been thought that efficient excited-state quenching channels effectively precluded adsorbate photochemistry on metals.[2,3] Second, metal carbonyls are the prototype (though by no means the best) system for the investigation of photoassisted chemical vapor deposition of metal layers.[4] Finally, photochemistry in metal carbonyls adsorbed on metal substrates is thought to be largely dominated by adsorbate localized excitation,[5−8] which is in contrast to the more common observation of a substrate-mediated, hot electron attachment, mechanism.[9−11] Thus the metal carbonyls afford the opportunity of investigating the effect of substrate morphology on adsorbate-mediated photochemical pathways. It has been established that surface roughening leads to an enhanced photochemical cross-section in some substrate-mediated photochemical reactions.[12−16] The enhancement mechanism involves surface plasmon excitation, which is allowed on roughened surfaces.[15,17] Surface plasmon excitation has also been suggested to have a role in adsorbate-mediated photochemistry, through a field enhancement mechanism,[18,19] and has been implicated in the photochemistry of adsorbed metal carbonyls.[20]

There are a number of previous studies of the photochemistry of $Fe(CO)_5$ adsorbed on a variety of surfaces.[1,21−33] Yates et al.[30,31] made extensive investigations of the photodissociation of $Fe(CO)_5$ on Ag(111) at two wavelengths, using postirradiation TD measurements. It was established that the primary photoreaction on irradiation between 250 and 400 nm was

SCHEME 1

$$x\mathrm{Fe(CO)_5(a)} + h\nu \rightarrow \mathrm{Fe}_x\mathrm{(CO)}_y\mathrm{(a)} + (5x - y)\mathrm{CO(g)}$$

and that the adsorbed photoproducts were essentially photoinactive. The cross-section for photochemistry in the adsorbate was reported to be similar to that found in the gas phase, suggesting that excited-state quenching does not compete strongly with photodissociation. However, a distinct surface effect was found, in an enhanced photodissociation cross-section at 365 nm for $Fe(CO)_5$ adsorbed directly on Ag(111), compared to that adsorbed on a decane spacer layer. This was ascribed to a red shift in the electronic spectrum for the directly adsorbed species.[30]

Sato et al. used infrared reflection absorption spectroscopy, in conjunction with temperature and coverage variation, to investigate the wavelength-dependent photochemistry of $Fe(CO)_5$ on both Ag(111)[20,32] and Au(111).[33] Vibrational spectroscopy revealed a number of species adsorbed on Ag(111). A chemisorbed form of $Fe(CO)_5$, which was not photoactive, was thought to have the square pyramidal structure.[33−35] The photoactive $Fe(CO)_5$ species was found to exist in two forms at 90 K, one assigned to $Fe(CO)_5$ directly adsorbed on Ag(111) and one to the multilayer. They[20] also recorded the action spectrum for the decarbonylation reaction (CO molecules per incident photon) as a function of wavelength, which exhibited a peak in the cross-section at 330 nm. The peak became more pronounced if $Fe(CO)_5$ was deposited on a monolayer of decane, a result that appears to be in disagreement with the cross-section

* To whom correspondence may be addressed (s.meech@uea.ac.uk).

10.1021/jp021286s CCC: $22.00
Published on Web 09/07/2002

measurements of Henderson et al.[30] The peak in the action spectrum and the associated distance dependence were attributed to a resonant coupling with the surface plasmon.[20]

The present measurements permit a more detailed analysis of the photodissociation of $Fe(CO)_5$ on Ag(111). Time-of-flight (TOF) mass spectrometry has been used to investigate the dynamics of the photodissociation reaction. It will be shown that the dynamics of the $Fe(CO)_5$ photoreaction depend on distance from, and interaction with, the substrate. PID measurements have been made in conjunction with measurements of the photochemical action spectrum. These permit an accurate assessment of the photochemical cross-section and contain important mechanistic information. All these measurements have been performed as a function of $Fe(CO)_5$ coverage, and for $Fe(CO)_5$ monolayers on decane spacer layers. All measurements are also reported as a function of surface roughening. The latter study allows an assessment of the role of surface plasmon resonance in the photochemical yield and action spectrum of $Fe(CO)_5$.

2. Experimental Section

The detailed description of the experimental set up has been given elsewhere.[36,37] The experiments were carried out in a UHV chamber pumped by a 250 $L \cdot s^{-1}$ turbomolecular pump. The background pressure in the chamber was better than 5×10^{-11} Torr (uncorrected ion gauge). The Ag single crystal, cut to $\pm 0.5°$ of the (111) plane and polished to a roughness <1 μm, was fixed by a tungsten wire loop between tungsten rods attached to a liquid nitrogen filled holder. The temperature of the crystal was measured by a chromel−alumel thermocouple wedged in a hole drilled in the side of the crystal. The base temperature of the assembly was 89 K. In the TD measurements the heating rate in was 3 $K \cdot s^{-1}$ and the entrance of the mass spectrometer shroud was placed approximately 1 mm from the crystal face. For the PID measurements the mass spectrometer entrance was 25 mm from the surface.

In the PID experiments irradiation was by a 100 W xenon arc lamp (PTI A1010) coupled with a monochromator of bandpass 12 nm. The TOF measurements were carried out using the third (355 nm) and fourth (266 nm) harmonics of a Continuum Surelite (SLI-10) Nd:YAG laser. The desorbed molecules were detected by the quadrupole mass spectrometer (Hiden HAL 2/301). For the time-of-flight measurements the amplified pulses from the channeltron detector were recorded by an EG&G Ortec MCS-Plus multichannel scaler (time resolution 2 μs/channel) synchronized with the laser Q-switch. The flight distance was 100 mm. The ion drift time (t_0) in the quadrupole mass spectrometer was determined (i) by reflecting the laser beam into the ion source and recording the onset of the ion signal for a particular mass, and (ii) from a series of measurements with different ion source potential settings.

A constant background and t_0 were subtracted from the time-of-flight spectra. After a conversion into the flux domain (dividing by the flight time) the spectra were fitted by a modified flux-weighted two-component Maxwell−Boltzmann distribution:[38]

$$F(t) = \sum_i A_i \frac{1}{t^5} \exp\left[-\frac{m}{2kT_i}\left(\frac{d}{t} - v_i\right)^2\right] \qquad i = 1, 2 \qquad (1)$$

where m is the mass of the desorbed particle, k is the Boltzmann constant, T_i is the equilibrium temperature, and v_i is a fitting parameter, essentially a stream velocity. v_i describes the deviation of the width of the distribution from that of the thermal one (negative for broader, positive for narrower). The mean translational energies $\langle E_i^{\text{trans}} \rangle$ were found by numerical integration of the result of the fit. The characteristic translational temperatures were calculated as $T_i^{\text{trans}} = \langle E_i^{\text{trans}} \rangle / 2k$.

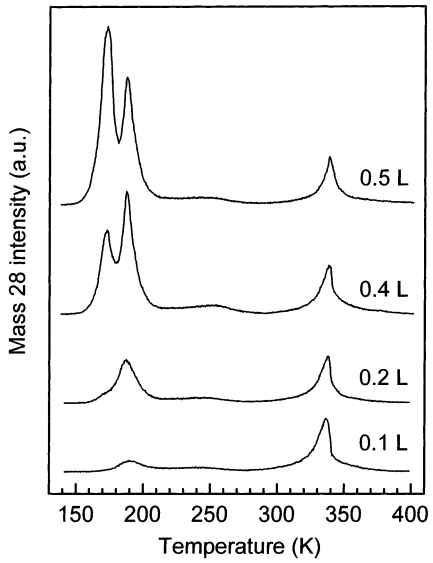

Figure 1. Mass 28 (CO) thermal desorption spectra from the Ag(111) surface for indicated doses of $Fe(CO)_5$ at 89 K.

Decane (99.9% anhydrous, Aldrich) and iron pentacarbonyl (99.999% Aldrich) were degassed by repeated freeze−thaw cycles. Directional dosers with calibrated leaks and positive shut-off valves were used (VTI) to dose the surface. The 1 monolayer dose of $Fe(CO)_5$ was prepared by depositing approximately 2 monolayers followed by careful flashing of the surface to 168 $\pm$ 1 K.

The Ag(111) surface was cleaned by cycles of argon ion sputtering (ion gun Phi Model 04-161) for 15 min with ions of 500 eV energy and a current of 1 $\mu A \cdot cm^{-2}$, and subsequent annealing at 700 K for 1 h. The rough surface was prepared by sputtering by 2 keV argon ions (5 $\mu A \cdot cm^{-2}$). The uniformity of the ion bombardment for the present geometry and the extent of surface roughening was assessed previously by Kidd et al.[15,39] The roughening protocol used followed the work of Goncher et al.[14] and Myli et al.[12,13] It has been established that ion bombardment creates bumps and craters of micron dimensions and features of the size of tens of nanometers.[12] However, the surface roughening is not sufficient to dramatically enhance the surface area, at least as judged by the integrated area of the monolayer peak in TD.

The data reported below are found to be more consistent with a kinetic scheme more complex that shown above. Simulations of PID on the basis of a proposed two-step kinetic scheme for the photochemistry of $Fe(CO)_5$ were performed using the IBM Chemical Kinetics Simulator (CKS) v1.01.[40] The validity of the CKS data output was verified by conducting comparative tests of CKS results to known exact solutions of two step uni-molecular and uni-bimolecular reaction schemes.[41] In each case excellent agreement was achieved between simulated and exact results. For each kinetic scheme the time dependence of CO desorption into the gas phase was simulated. The CO evolution curves were fitted to a sum of exponentials function, differentiated and compared with the experimental PID data.

3. Results and Discussion

3.1. Thermal Desorption. In Figure 1 the mass 28 TD data for Ag(111) surfaces exposed to increasing amounts of $Fe(CO)_5$

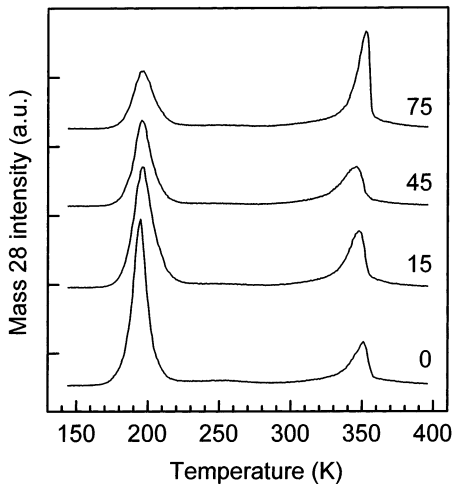

Figure 2. Mass 28 (CO) thermal desorption spectra of 1 monolayer of $Fe(CO)_5$ on Ag(111) after exposure to 345 nm radiation of power density 8.5 mW·cm^{-2} for 15, 45, and 75 s. 0 denotes the nonirradiated surface (the light beam has not covered the whole surface of the crystal).

at 89 K are shown. Three peaks are evident at 172, 187, and 336 K, with an additional broad and very weak signal between 210 and 260 K. The 336 K site is the only one seen at low exposures, and its mass 28 signal is not accompanied by desorption of Fe-containing species. With increasing exposure, the peak at 187 K is observed, with identical shapes at both mass 28 and 56. This peak is therefore assigned to molecular desorption. The 187 K peak saturates for exposures of 0.3−0.4 langmuir, and the final 172 K peak appears above 0.3 langmuir and increases with increasing exposure. The latter peak is assigned to formation of multilayers.

In Figure 2 the effect of irradiation at 345 nm on the TD spectra of a monolayer of $Fe(CO)_5$ on Ag(111) is shown. The area of the molecular desorption peak decreases monotonically, and broadens slightly, with increasing irradiation time. The 336 K peak increases in an inverse fashion. The product signal at 336 K does not subsequently decrease under prolonged or more intense irradiation. The photochemical reaction is accompanied by the appearance of CO in the gas phase, but not Fe. This is consistent with a photodecarbonylation reaction (Scheme 1) to yield an adsorbed $Fe_x(CO)_y$ photoproduct, which itself undergoes thermal decomposition, yielding CO, but not further photodissociation.

The data of Figures 1 and 2 are wholly consistent with the previous observations of Henderson et al.[30] and with the report of Sato and Tanaka,[20] although in the latter case they observed a broader and more complex high-temperature TD trace than is seen in Figure 1. These data are included here to provide a reference for later measurements.

In Figure 3 the mass 28 TD signal arising from Ag surfaces subjected to argon ion sputtering for different times are shown. The initial exposure was 0.6 langmuir (approximately 3 monolayers) of $Fe(CO)_5$ in each case. The most significant changes are observed in the shape and amplitude of the peak initially observed at 336 K. The temperatures of maximum desorption and peak areas (relative to the monolayer signal) are presented in Table 1. Essentially the effect of roughening is to increase the relative amplitude of the high temperature peak and to shift it to a slightly lower temperature. On an extensively roughened surface (90 min bombardment, which is expected to lead to a microscopically rough surface with nanometer- to micron-sized bumps[12]) the high-temperature site is enhanced by a factor of ∼2, compared with the Ag(111) surface (Table 1).

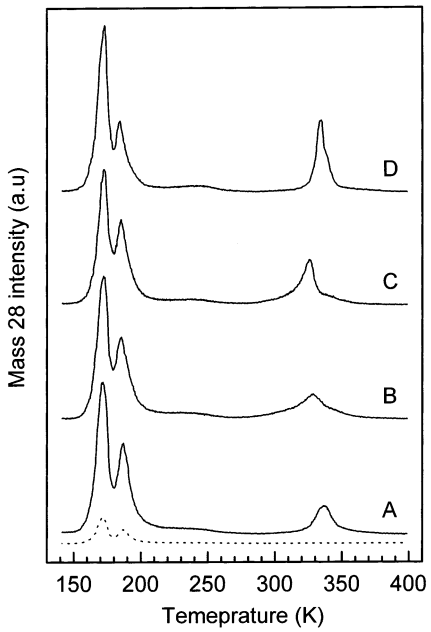

Figure 3. Mass 28 thermal desorption spectra after 0.6 langmuir dose of $Fe(CO)_5$ at 89 K on Ag(111) surfaces roughened by Ar^+ ion sputtering (2 keV, 5 μA·cm^{-2}). Sputtering times: 3 min (B), 45 min (C), and 90 min (D), respectively. (A) denotes the nonsputtered (111) surface. The dashed line is mass 56 (Fe) corresponding to the molecular desorption of $Fe(CO)_5$.

TABLE 1: Peak Temperatures and Areas in the TPD Spectra of 0.6 Langmuir of $Fe(CO)_5$ Adsorbed on a Flat Ag(111) Surface and Surfaces Roughened by Ar^+ Ion Sputtering.

surface sputtering time[a] (min)	physisorbed		chemisorbed	
	temp (K)	area	temp (K)	area[b]
(111)[c]	171, 187	6.88	336	1.00
3	172, 185	5.53	328	1.63
45	173, 185	5.14	326	1.84
90	172, 184	5.28	334	1.83

[a] Ar^+ 2 keV, 5 μA·cm^{-2}. [b] Areas relative to the high-temperature peak on the flat (111) surface. [c] Flat (111) surface.

On the basis of the preceding data it is safe to assign the 172 and 187 K peaks to multilayer and physisorbed monolayer of $Fe(CO)_5$, respectively. Both features are retained on the roughened surface. It is not possible to make a definitive assignment of the 336 K signal from TD data alone. However, its appearance thermally and photochemically and its appearance as a function of surface roughness, at approximately the same temperature and with a similar profile, point to a common species. On the nonirradiated Ag(111) surface this species may arise either from direct dissociative adsorption of $Fe(CO)_5$ or from thermal decomposition of $Fe(CO)_5$ adsorbed at defect sites. The infrared data of Sato and co-workers suggest a thermal decomposition, arising from the chemisorbed $Fe(CO)_5$ state that they observed.[42] That the same state is generated by irradiation, which yields CO as a photoproduct, supports an assignment to $Fe_x(CO)_y$ with $(y/x) < 5$ (Figure 2). The $Fe(CO)_4$ species is an obvious possibility, although vibrational spectroscopy suggests that more than one photoproduct is formed on Ag(111).[20] The enhancement of the 336 K site on surface roughening (Figure 3) is consistent with the thermal formation of this species at defect sites.

In Figure 4 postirradiation TD data for multilayer exposures are shown as a function of surface roughness (sputtering time). Significant differences between photochemistry in the mono-

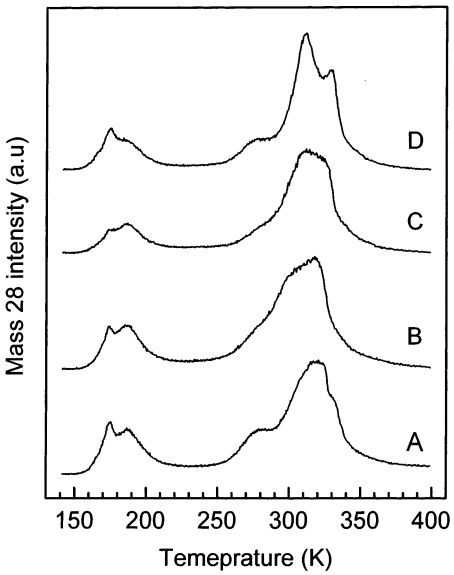

Figure 4. Postirradiation mass 28 (CO) thermal desorption spectra of 3 monolayers of $Fe(CO)_5$ on Ag(111) exposed to Ar^+ ion sputtering (same conditions as Figure 3) for 3 min (B), 45 min (C), and 90 min (D), respectively. (A) denotes the nonsputtered (111) surface. Surface was irradiated by 345 nm radiation of power density of 8.5 mW·cm^{-2} for 170 s (the light beam has not covered the whole surface of the crystal).

and multilayers are immediately apparent, from a comparison of the data for the unroughened irradiated surface in Figure 4 (trace A) with that for the irradiated surfaces in Figure 2. Most obviously there is a richer range of photoproducts following multilayer photolysis, leading to a complex CO desorption profile, comprising at least three peaks between 250 and 350 K. Thus, the dominant part of the photoproduct desorption for multilayers occurs at temperatures below that for the photoproducts formed on monolayer photolysis (336 K). No Fe desorption was seen in TD at the higher temperature, suggesting decomposition of the photoproducts to leave Fe on the surface. In addition, the higher temperature TD profiles were unaffected by prolonged irradiation, suggesting that the multilayer photoproducts are also themselves photoinactive. The low temperature 160−220 K TD profiles show that both multilayer and monolayer species are photoactive, so direct contact with the surface is not a prerequisite for photodecomposition. It is also apparent that the residual population in the monolayer after irradiation has a broader TD profile than is observed before irradiation (compare Figure 4 and Figure 1). This suggests that the photoproducts formed following multilayer photolysis perturb the residual physisorbed $Fe(CO)_5$. Compared to the large changes between the mono- and multilayer coverages, the effect of surface roughening on the postirradiation TD spectra is slight (Figure 4B − D).

In Figure 5 the TD spectra for a submonolayer coverage of $Fe(CO)_5$ on 10 monolayers of decane are shown, pre- and postirradiation. For the unirradiated surface only a single peak, associated with molecular desorption, is seen. The effects of irradiation are similar to those in the multilayer case (Figure 4). The residual monolayer peak is broadened, and no further desorption of CO is detected up to 330 K. Above 330 K a broad multicomponent CO profile is again observed, with no accompanying Fe desorption. Thus, the broadening of the high-temperature CO TD is not exclusively a result of multilayer photolysis, but rather a consequence of $Fe(CO)_5$ being separated from the Ag(111) surface. The similar behavior for both multilayers and the submonolayer deposited on decane suggests

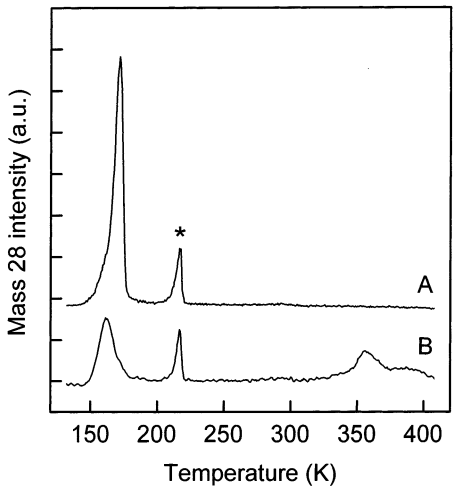

Figure 5. Mass 28 (CO) thermal desorption spectra of 0.8 monolayer of $Fe(CO)_5$ dosed at 89 K on Ag(111) covered by 10 monolayers of *n*-decane: (A) nonirradiated surface; (B) surface irradiated by 266 nm light for 300 s at 10 mW·cm^{-2} (the light spot has not covered the whole crystal). The peak marked with an asterisk comes from the desorption of *n*-decane.

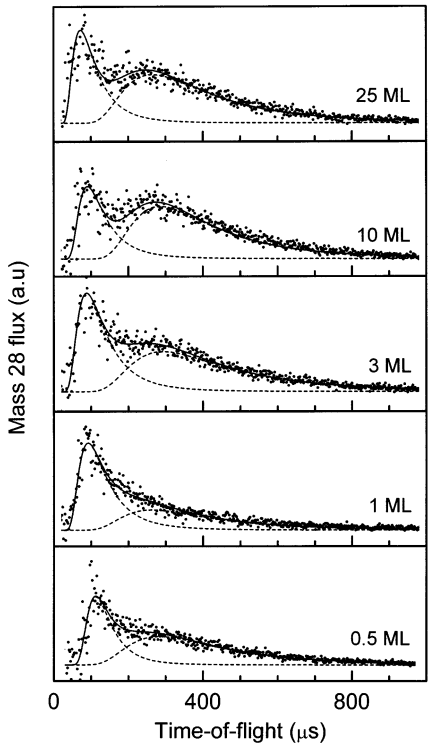

Figure 6. Time-of-flight spectra of CO from $Fe(CO)_5$ adsorbed on Ag(111) at 89 K obtained by 355 nm irradiation (5 ns pulses, 0.2 mJ·cm^{-2}).

the existence of interadsorbate interactions on the decane film that are absent in the monolayer on Ag(111).

3.2. Time-of-Flight Mass Spectrometry. The mass 28 time-of-flight profiles observed for $Fe(CO)_5$ on Ag(111) irradiated by 5 ns pulses at 355 nm are shown as a function of coverage in Figure 6. Although the data are noisier than we have seen for other photoreactions,[37] due to the high background of CO in the chamber, the qualitative trends are clear. The profiles reveal both fast and slow components. The data are well fit by a sum of two modified Maxwell−Boltzmann distributions, and the results of this analysis are presented in Table 2. The fit yields a characteristic translational temperature for the slow component

TABLE 2: Summary of CO Time-of-Flight Spectra Obtained by 355 and 266 nm Irradiation of $Fe(CO)_5$ Adsorbed on Ag(111) Surface

	355 nm			266 nm		
	temp[b] (K) component		ratio[c]	temp[b] (K) component		ratio[c]
coverage (monolayer)[a]	fast	slow	fast/slow	fast	slow	fast/slow
0.5	890 ± 82	77 ± 7	0.78 ± 0.09	830 ± 72	78 ± 7	0.90 ± 0.07
1	810 ± 69	103 ± 12	1.40 ± 0.08	800 ± 42	80 ± 17	1.00 ± 0.06
3	810 ± 70	70 ± 8	0.75 ± 0.05	960 ± 80	87 ± 9	0.46 ± 0.04
10	990 ± 85	78 ± 6	0.43 ± 0.07	940 ± 96	80 ± 8	0.44 ± 0.06
25	1150 ± 90	83 ± 7	0.43 ± 0.06	1130 ± 88	87 ± 7	0.51 ± 0.05
0.8 /10 monolayers of decane				909 ± 82	78 ± 10	0.50 ± 0.04

[a] Coverage in monolayers derived from temperature-programmed desorption data of the nonirradiated surface. [b] Characteristic temperature derived from the mean translational energy: $T = \langle E_{trans} \rangle / 2k$. [c] Ratio of intensities obtained by numerical integration of the two-component modified Maxwell−Boltzmann distribution fits.

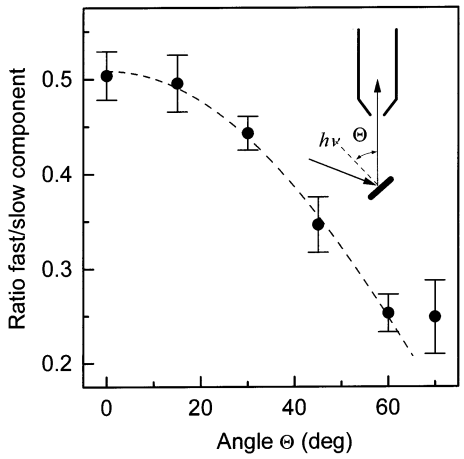

Figure 7. Angular dependence of the ratio of the fast and slow components of the CO TOF spectra from 266 nm irradiation of 20 monolayers of $Fe(CO)_5$ on Ag(111) at 89 K. The dashed curve is a least-squares fit of the data by a function $A \cos^n(\theta)$. The fit gives $n = 1.03$. The inset indicates the experimental setup.

equal (within the error of the fit) to the substrate temperature (89 K). This result strongly suggests a thermal equilibration of the CO product prior to desorption. On the other hand the fast component is characterized by a considerable translational temperature and is ascribed to CO produced by photolysis and directly entering the gas phase with minimal interaction with the surface. Essentially identical data were obtained for photolysis at 266 nm (Table 2).

The assignment of the two distributions observed to a thermalized and photochemical channel was supported by an investigation of the angular dependence of the time-of-flight profile. This was achieved by rotating the sample about its axis, leaving the geometry of the photolysis source and mass spectrometer unchanged (inset to Figure 7). Absolute measurements would require a number of geometry dependent corrections. To overcome this problem, we report the relative weights of the fast and slow component as a function of sample rotation angle. The results are shown in Figure 7, for photolysis at 266 nm. The expectation is that a thermalized photoproduct will desorb with a cos θ distribution.[43] In contrast, for an adsorbate photodissociation reaction the angular distribution is often observed to have a $\cos^n \theta$ distribution, with $n > 1$.[44] The ratio of fast to slow amplitudes is plotted in Figure 7 as a function of the angle. The data are well fit by a cos θ function. This is consistent with the assignment of the two time-of-flight distributions to thermal and direct photochemical channels, the latter having a $\cos^n \theta$ distribution, with $n = 2$.[45] Two-component, photochemical and thermal, time-of-flight distributions were previously observed for photolysis of $Mo(CO)_6$ on Si(111).[46] The rotational temperature of the slow component was measured, and it reflected the surface temperature.

From Figure 6 and Table 2 it is clear that the ratio of fast (photolysis) to slow (thermal) component is coverage dependent. For a coverage of 1 monolayer the weights of the two components are approximately equal, whereas for coverages in excess of 1 monolayer a ratio of <0.5 is observed, independent of layer thickness (up to at least 25 monolayers). Thus the thermalized component is enhanced at the onset of multilayer coverage but does not increase further with additional layers. In addition, for submonolayer coverages of $Fe(CO)_5$ on a decane spacer layer the ratio of photochemical to thermalized CO yield is approximately 0.5. Thus, the submonolayer on the decane system is more similar to multilayer $Fe(CO)_5$ than to a monolayer on Ag(111), as was also observed in TD.

A fast component in the TOF distribution is expected, on the basis of the clear observation in TD of a photochemical decarbonylation reaction on the surface, and of data available concerning the gas-phase photochemistry of $Fe(CO)_5$, which shows that excitation of low lying electronic transitions results in dissociation to yield CO.[47]

There are at least two plausible explanations for the appearance of a thermalized component. First, photolysis of the symmetrical $Fe(CO)_5$ may lead to CO being ejected toward the surface. For such a product to eventually be detected in the gas phase it is likely to undergo a number of collisions with the surface and, especially in the case of multilayer coverage, with coadsorbates. These collisions would lead to thermalization before desorption. Such a model was invoked by Buntin et al. in their study of $Mo(CO)_6$ photolysis on Si(111).[46] Alternatively, it has been suggested, in both matrix and surface photochemical studies, that the primary photoproduct, $Fe(CO)_4$, may undergo further reactions with $Fe(CO)_5$, to yield dimeric or polymeric species.[33,47] These secondary reactions may act as an additional source of CO, and it is expected that the CO so produced would be desorbed with a translational temperature reflecting that of the substrate. We note that in the postirradiation TD data for both multilayer coverages (Figure 4) and the Ag(111)/decane/$Fe(CO)_5$ system (Figure 5) there is evidence for the production of multiple products, which may arise from such secondary reactions. We will return to the origin of the thermalized CO component after describing the PID measurements.

3.3. Photon-Induced Desorption. In PID the flux of the photoproduct in the gas phase is monitored under continuous irradiation. For the reaction in Scheme 1 the flux is given by

$$\frac{dn_{CO}}{dt} = k n_{Fe(CO)_5} = n^0_{Fe(CO)_5} k e^{-kt} \qquad (2)$$

in which n_x is the number density of species x and $k = \sigma f$, where

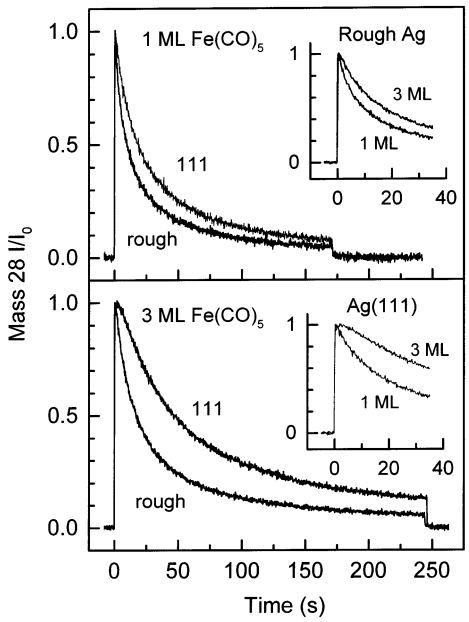

Figure 8. Photoinduced desorption of CO from $Fe(CO)_5$ on Ag(111) and surface roughened by 90 min sputtering by Ar^+ ions. The upper and lower panels show the PID traces for a 1 monolayer and a 3 monolayer $Fe(CO)_5$ coverage, respectively. In the insets the PID signals for different coverage on identical surfaces are compared. The power density of the 345 nm radiation was 5.2 mW• cm^{-2}. The temperature was 89 K.

TABLE 3: Initial Photodesorption Cross-Section of 1 and 3 Monolayers of $Fe(CO)_5$ on Ag(111) and Ag Surfaces Roughened by Ar^+ Ion Sputtering for 345 nm Radiation

surface roughening time (min)	cross-section (cm^2)	
	1 monolayer	3 monolayer
(111)[a]	$(3.8 \pm 0.6) \times 10^{-18}$	$(1.3 \pm 0.5) \times 10^{-18}$
3	$(3.1 \pm 0.8) \times 10^{-18}$	$(2.5 \pm 0.5) \times 10^{-18}$
45	$(4.7 \pm 0.6) \times 10^{-18}$	$(3.2 \pm 0.6) \times 10^{-18}$
90	$(4.3 \pm 0.5) \times 10^{-18}$	$(2.1 \pm 0.5) \times 10^{-18}$

[a] Flat undamaged (111) surface.

σ is the photochemical cross-section and f is the photon flux. Hence, for the simple first-order scheme a single-exponential PID is predicted, with decay constant equal to k and an initial amplitude equal to the product of k and the initial coverage. The PID measurements for 1 and 3 monolayers of $Fe(CO)_5$ on Ag(111) and on extensively roughened silver are compared in Figure 8. It is noticeable that the data deviate from the expected single exponential time dependence (eq 2). This may arise from a number of factors, either fundamental, such as Scheme 1 being an inappropriate description of the true desorption mechanism, or instrumental, for example, an inhomogeneous irradiation beam. The PID data were all well described by a sum of two exponential terms. Only the fastest, initial, relaxation time has been used to calculate the cross-sections, which are shown in Table 3.

Three qualitative results are clearly seen in Figure 8, and supported quantitatively by the initial rate analysis in Table 3. First, when the surface is roughened, the photochemical cross-section increases. Second, when the thickness of the layer is increased the cross-section decreases. Third, the enhancement due to surface roughness is smaller for the thicker layer. Finally, it is noted that the photochemical cross-section is, in agreement with earlier measurements,[30,31] large compared to that seen for other adsorbates and close to the gas-phase cross-section. This is consistent with an adsorbate-mediated photochemical mechanism, in which direct dissociation competes effectively with excited-state quenching.

TABLE 4: Photodesorption Cross-Section for 345 nm Radiation of 0.8 Monolayer of $Fe(CO)_5$ Adsorbed on Ag(111) and Roughened Ag Surfaces

surface roughening time (min)	cross-section (cm^2)	
	fast component	slow component
(111)[a]	$(3.4 \pm 0.6) \times 10^{-18}$	$(6.6 \pm 0.6) \times 10^{-19}$
(111)/10 monolayers of decane		$(6.4 \pm 0.7) \times 10^{-19}$
90	$(3.8 \pm 0.7) \times 10^{-18}$	$(9.0 \pm 0.9) \times 10^{-19}$
90/2 monolayers of decane		$(7.2 \pm 0.8) \times 10^{-19}$
90/4 monolayers decane	-	$(6.5 \pm 0.4) \times 10^{-19}$
90/10 monolayers of decane	-	$(6.8 \pm 0.5) \times 10^{-19}$

[a] Flat undamaged (111) surface.

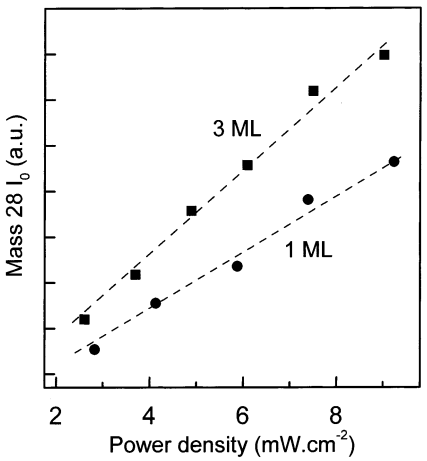

Figure 9. Dependence of the initial CO PID intensity on the power density for 345 nm irradiation: (■) 3 monolayers of $Fe(CO)_5$ on Ag(111); (●) 1 monolayer of $Fe(CO)_5$ on Ag(111).

The observation of a decreasing cross-section with increasing distance from the surface is an unexpected result for an adsorbate-mediated photodissociation. It is expected that the rate of excited-state quenching decreases with increasing distance from the metal substrate,[3,11] allowing photochemistry to compete more effectively. However, our result is in agreement with the observation of Henderson et al. at 365 nm.[30] Conversely, the result in Figure 8 is at odds with the measurement of Sato and Tanaka, who reported an enhanced cross-section for photodecarbonylation when $Fe(CO)_5$ was separated from the substrate by a decane spacer layer.[20] We have recorded the PID for $Fe(CO)_5$ separated from the surface by a decane spacer layer. The result is again a decrease in cross-section when the adsorbate is separated from the Ag(111) surface (the data are shown later, in Figure 11 and Table 4).

The apparent disagreement among reports of the distance dependent cross-section may be resolved by considering how the measurements were performed. Here the initial slope of the PID trace for CO desorption has been measured, which directly yields the cross-section for a given photon flux (eq 2). Henderson et al. recorded the residual coverage of $Fe(CO)_5$ as a function of irradiation time, using postirradiation TD. Thus the rate of $Fe(CO)_5$ consumption is directly determined, and a log plot for known irradiation conditions yields σ directly. Sato and Tanaka measured the initial rise of CO concentration in the gas phase at the onset of irradiation.[20] This measurement yields σn^0 (eq 2). We have also reproduced the initial rise measurement, as a function of irradiation intensity. The data for 1 and 3 ML of $Fe(CO)_5$ on Ag(111) are shown in Figure 9. On the basis of this measurement an enhancement of 1.4 times

in the cross-section for the thick layer is obtained, close to the enhancement reported by Sato and Tanaka.[20] This is clearly at odds with the slope of the PID, although these were recorded under identical conditions (Figure 8). The disagreement is resolved if it is allowed that there are more photoactive sites in the multilayer system than in the monolayer. Specifically, using the data in Table 3, agreement requires that the ratio $n_{3ML}{}^0/n_{1ML}{}^0 = 4$. The TD spectra show that there are indeed photoinactive sites in the first layer, which thermally populate the state, leading to desorption of CO at 336 K. This alone could not account for a factor of 4 (see Table 1). However, the above analysis assumes a simple first-order mechanism (Scheme 1). There is ample evidence, from the multicomponent TOF traces and the multiexponential PID, that the $Fe(CO)_5$ photodissociation on Ag(111) may be more complex that Scheme 1 suggests. For example, a range of sites with different cross-sections might be sufficient to account for the different observations; we return to the possibility of more complex kinetic schemes in section 3.5.

Because the slope extracted from the PID data (Figure 8) is independent of the initial coverage, it may be accepted (within the limits of the first-order model) that the photochemical cross-section at 345 nm decreases with increasing coverage beyond 1 monolayer and with distance from the surface. Henderson et al. obtained the same result and tentatively ascribed it to a red-shifted electronic spectrum in the monolayer, leading to enhanced absorption.[30] To test this idea the wavelength dependence of σ (the photochemical action spectra) has been measured for monolayer and multilayer coverage, and as a function of surface roughness. The results are presented in Figure 10. In all cases the action spectra reveal a broad band, with an onset at about 410 nm (2.8 ± 0.2 eV) and a maximum at 335 nm (3.7 ± 0.2 eV), followed by a rise at 310 nm (4 eV). Within the experimental error, the action spectra measured here are independent of coverage and surface roughness. In particular, the action spectrum for 1 and 9 monolayers are overlapped (trace A). Thus, there is no evidence for a large spectral shift associated specifically with the first layer, so this cannot be the mechanism of the large cross-section in the directly adsorbed layer (Figure 8) and another explanation must be sought. Possibilities include the following. First, a short-range enhancement of the optical field may enhance the cross-section in the first layer. Such an explanation was considered earlier by So and Ho to explain enhanced dissociation in the action spectrum for $Mo(CO)_6$ photodissociation on Ag(111) at 325 nm.[48] The difficulty with this explanation is that a resonant enhancement is predicted at the wavelength of the d band to Fermi level transition, <330 nm, whereas the enhancement in the $Fe(CO)_5$ photodissociation operates at 345 nm (above) and 360 nm.[30] An alternative explanation for an enhanced cross-section in the first layer is that the molecules directly adsorbed on silver undergo a structural perturbation that results in an intrinsically higher cross-section. That the first and subsequent layers are distinct was shown by Sato and Tanaka, who noted that the infrared absorption associated with the species desorbing at 187 K is different from that of the multilayer.

3.4. Photochemical Enhancement on Roughened Surfaces. That the action spectrum for $Fe(CO)_5$ photodissociation is perturbed by adsorption is evident from a comparison with the gas-phase absorption spectrum. In the adsorbate a peak in the cross-section is observed around 335 nm (Figure 10), whereas in the gas-phase absorbance rises monotonically from 350 nm to the first peak at 250 nm, assigned to a metal−ligand charge-transfer band;[49] there is a weak underlying electronic state at

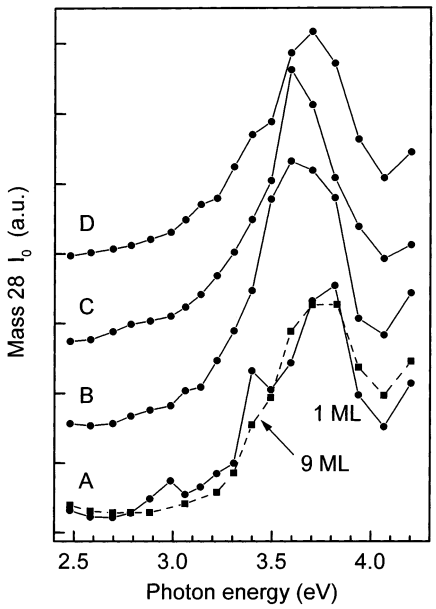

Figure 10. Action spectra for the desorption of CO from 1 monolayer of $Fe(CO)_5$ adsorbed on the Ag(111) surface (A) and the Ag(111) surface roughened by Ar^+ ion sputtering for 3 min (B), 45 min (C), and 90 min (D). The dashed line is for a 9 monolayer dose of $Fe(CO)_5$ on the (111) surface. The temperature was 89 K.

330 nm, assigned to a metal-localized transition,[50] but this does not yield the distinct peak seen in the adsorbate.

The assignment of the 335 nm peak has been a subject of some discussion. A similar profile was seen in the action spectrum of $Mo(CO)_6$ on Ag(111), and assigned to electron spill out effects.[48] However, such effects are short range, whereas the peak in $Fe(CO)_5$ persists for multilayer species (Figure 10). The 335 nm peak has also been assigned to surface-plasmon-enhanced photodissociation.[20] It was proposed that the surface plasmon excitation, which is forbidden on a flat (e.g., Ag(111)) surface, becomes allowed through the presence of defects. Resonance between the applied optical field and the surface plasmon resonance (which is observed at 350 nm in isolated nanonmeter-sized silver spheres) leads to enhanced field strength at the surface, hence an enhanced photochemical cross-section. The mechanism proposed is analogous to surface-enhanced Raman scattering, except that the effect may be smaller due to the competitive effect of excited-state quenching.[18,19] This mechanism has the merits of yielding both resonant behavior and the long-range effect observed. In fact, an enhanced cross-section with increasing distance from the surface was reported, on the basis of the initial rise in the PID.[20] This is consistent with models of surface-enhanced adsorbate-mediated photochemistry, where a maximum cross-section some distance above the surface arises from a balance between the decreasing field enhancement and increasing excited-state lifetime with increasing distance.[51] However, as discussed above, that conclusion is not supported by measurements based on the decay of the PID, where a smaller cross-section is observed for the thick films.

In our earlier study of surface-plasmon-enhanced *substrate-mediated* photochemistry it was reported that an enhancement at the plasmon frequency was only observed on extensively roughened surfaces.[15] In light of this we have recorded the action spectra for $Fe(CO)_5$ photodissociation as a function of surface roughness. These data are included in Figure 10. It is readily seen that there is no significant difference between action spectra recorded on the smooth and annealed Ag(111) surface, and the silver surface subjected to extensive roughening by energetic

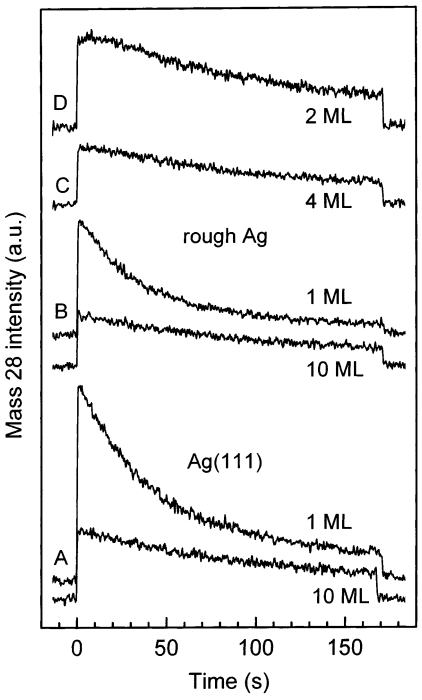

Figure 11. Photoinduced desorption of CO from 0.8 monolayer of $Fe(CO)_5$ dosed on *n*-decane-covered (2, 4, and 10 monolayer) Ag(111) and an Ar^+ sputtered surface (2 keV, 5 $\mu A \cdot cm^{-2}$, 90 min): (A) (111) surface bare (upper trace) and 10 monolayer of *n*-decane (lower trace); (B) roughened surface bare (upper trace) and 10 monolayer of *n*-decane (lower trace); (C) roughened surface, 4 monolayer of *n*-decane; (D) roughened surface, 2 monolayer of *n*-decane. The PID traces obtained without the spacer layer are shown for comparison.

argon ions. The latter procedure is known to generate microscopic features on the surface that will certainly support plasmon excitation.[12] From these data we conclude that there is no evidence that the maximum observed in the photodissociation cross-section at 335 nm arises from surface plasmon excitation. It is proposed instead that the peak that is seen in the action spectrum arises from a perturbation to the electronic structure of $Fe(CO)_5$ when it is condensed on the silver surface.

The distance dependence of the cross-section for submonolayers of $Fe(CO)_5$ deposited on decane spacer layers has also been investigated through PID. Irradiation was at 335 nm. The data are shown in Figure 11. First, for the Ag(111) surface, directly adsorbed $Fe(CO)_5$ clearly has a larger cross-section than $Fe(CO)_5$ adsorbed on a thick (10 monolayer) decane film. This is consistent with the enhanced cross-section for directly adsorbed species, described earlier. This factor also operates on a heavily roughened silver surface; the cross-section of the directly adsorbed layer is larger than that of the adsorbate separated from the surface by a spacer layer. By observing PID on the heavily roughened surface, as a function of the thickness of the decane spacer layer, we see that the cross-section is always smaller than that for the directly adsorbed $Fe(CO)_5$ and is only a weak function of spacer layer thickness. Thus there is no evidence from PID data recorded as a function of thickness of the decane layer, for surface-plasmon-enhanced adsorbate-mediated photochemistry in $Fe(CO)_5$. This conclusion is at odds with the data of ref 20. We believe the origin of this discrepancy lies in the different methods used to record the data, as already discussed in section 3.3, above.

Returning to the PID data shown in Figure 8 and Table 3, it is seen that when the same adsorbate system is compared on rough and smooth surfaces there is evidence for a weakly surface-enhanced cross-section for adsorbate photochemistry. For example, monolayer $Fe(CO)_5$ directly adsorbed on the silver surface clearly has a larger cross-section for photodissociation when the surface is roughened (Figure 8). The same is true for the 3 monolayer $Fe(CO)_5$ surface. The enhancement factor ($\sigma_{rough}/\sigma_{smooth}$) is larger for the multilayer, although the absolute cross-section decreases between the monolayer and thick film. Thus, these data suggest roughness-enhanced photochemistry at 335 nm, although the first layer enhancement serves to obscure distance dependent enhancements due to surface roughening. The fact that the effect is seen on a thick (3 monolayer) layer suggests that the effect is long range. This is consistent with a mechanism involving enhanced field strength due to resonance with the surface plasmon. However, the effect is very small, less than a factor of 2, which is much smaller than is seen for the surface-enhanced substrate-mediated photochemistry[15] and insufficient to account for the 335 nm peak in the action spectrum (Figure 10).

3.5. Kinetic Model for $Fe(CO)_5$ Photochemistry. In setting up a kinetic model to describe the photochemistry of $Fe(CO)_5$ on silver, three factors must be taken into account. First, the TOF data show that both translationally hot and thermally equilibrated CO are produced in the gas phase, the latter being more prominent for multilayer coverage (Figure 6). Second, PID show that the photochemical cross-section decreases with increasing coverage (Figure 8) and distance from the surface (Figure 11), whereas the yield of CO increases (Figure 9). Finally, photolysis of a thick sample results in the observation of a richer range of photoproducts in TD than monolayer photolysis (Figure 4). None of these results is readily reconciled with a simple first-order reaction (Scheme 1).

An obvious extension to the first-order model is to allow the possibility of trapping of CO by the film, and its subsequent release after thermalization. Because $Fe(CO)_5$ is symmetrical, it is reasonable to expect that CO may be ejected in any direction. The fraction directed toward the surface will undergo collisions with the surface and coadsorbates before desorption into vacuum. From the TOF data (Figure 8) it is seen that the yield of thermalized CO increases for both multilayer coverage and adsorption of submonolayer $Fe(CO)_5$ on decane spacer layers. This is also reasonable, as trapped CO may most readily be generated by photodissociation of $Fe(CO)_5$ trapped in the film, or, in the case of the spacer layer, in $Fe(CO)_5$ clusters. However, although the trapping model accounts nicely for the TOF observations, and possibly the coverage dependent PID data, there remain some experimental results for which it does not account. First, it fails to reproduce the broader distribution of photoproducts in multilayers, observed in TD (Figure 4) and infrared spectroscopy.[52] Second, it does not account for the apparent increase in yield of CO per photon at higher coverage (Figure 9).

A two-step mechanism is proposed to account for these latter observations. The first step is direct photolysis to yield translationally hot CO in the gas phase, as in Scheme 1. This is followed by a dark reaction between the $Fe(CO)_4$ product and the reactant, to yield a second product, and an additional, thermalized, CO molecule for each absorbed photon:

$$Fe(CO)_5 + h\nu \rightarrow Fe(CO)_4 + CO_g \qquad k_1$$

$$Fe(CO)_4 + Fe(CO)_5 \rightarrow Fe_2(CO)_8 + CO_g \qquad k_2$$

The second step becomes significant at multilayer coverage and on a decane spacer layer. Although this kind of consecutive parallel reaction is not exactly solvable,[53] it may be solved numerically. This has been done using the CKS package[40] to

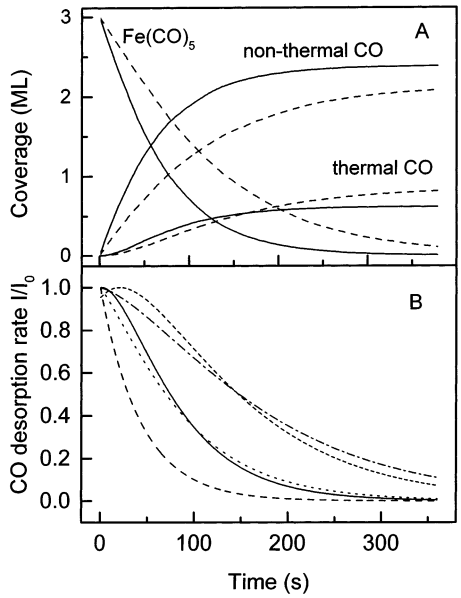

Figure 12. Simulation results for the proposed two step mechanism. (A) Thermal and nonthermal CO desorption curves for the multilayer case. Solid line $k_1 = 0.0115\ s^{-1}$, dashed line $k_1 = 0.0057\ s^{-1}$ ($k_2 = 0.003\ cm^2\ s^{-1}$ for both cases). Also shown, the decay curves of $Fe(CO)_5$. (B) Predicted CO desorption rate curves generated from the proposed two-step mechanism. Monolayer: dotted line $k_1 = 0.023\ s^{-1}$. Multilayer: solid line $k_1 = 0.015\ s^{-1}$, $k_2 = 0.003\ cm^2\ s^{-1}$; dashed line $k_1 = 0.015\ s^{-1}$, $k_2 = 0.001\ cm^2\ s^{-1}$; dash−dot line $k_1 = 0.0057\ s^{-1}$, $k_2 = 0.003\ cm^2\ s^{-1}$; dash−dot-dot line $k_1 = 0.0057\ s^{-1}$, $k_2 = 0.001\ cm^2\ s^{-1}$.

calculate the evolution of CO, from which the PID data are then calculated, as described earlier. The choice of k_1 was guided by the initial slope of the PID, and different values of k_2 were selected to simulate the PID. If k_1 is kept constant as coverage is increased, the PID predicted by this scheme is faster at higher coverage, in contradiction to observations. However, if the idea of an enhanced cross-section in the first layer is retained, the experimentally observed trends in the PID are readily reproduced, as can be seen from Figure 12. It is interesting to note that the PID data predicted exhibit a rise at early times. There are hints of this behavior in some experimental data, most notably for adsorption on decane spacer layers, Figure 11. Thus this simple kinetic scheme is at least qualitatively consistent with the experimental observations on the Ag(111) surface as a function of coverage. Of course more elaborate kinetic schemes could be produced to yield quantitative agreement, but there is insufficient experimental data, particularly with regard to the product distribution, against which to test them.

4. Conclusions

The photochemistry of $Fe(CO)_5$ on silver has been studied as a function of coverage and distance from the surface, using a variety of methods. The photochemistry is adsorbate mediated, but perturbed by the substrate. The photochemical mechanism is more complex than first order. The effect of even very extensive surface roughening is slight. More specific conclusions are as follows.

1. Photodissociation of $Fe(CO)_5$ proceeds on the Ag(111) surface to yield CO in the gas phase. The cross-section is comparable to that found for gas-phase photolysis. The action spectrum does not approximate the absorbance of the silver substrate. Taken together, these data suggest a photodissociation mechanism involving electronic excitation of the adsorbate, rather than a substrate-mediated hot electron attachment mechanism. The photoproduct generated is not itself photoactive but undergoes thermal decomposition.

2. Photodissociation of directly adsorbed $Fe(CO)_5$ yields a single product peak in TD at 335 K. However, the photochemical products formed in multilayers, and submonolayers adsorbed on a decane spacer layer, show much more complex profiles in their TD spectra.

3. Time-of-flight measurements show that CO is generated by two channels, leading to translationally hot and thermalized products, respectively. The latter channel increases in significance for multilayers and for $Fe(CO)_5$ adsorbed on a decane spacer layer. The former channel is ascribed to direct photodissociation yielding gas-phase CO with little or no interaction with the surface. The thermalized channel may indicate either trapping of CO prior to desorption, or dark reactions proceeding on the surface.

4. Photon-induced desorption measurements show that the photodissociation cross-section is larger for $Fe(CO)_5$ directly adsorbed on Ag than it is when it is separated from the surface. This result is true for both multilayers and for a submonolayer adsorbed on decane. This is ascribed to a structural perturbation of $Fe(CO)_5$ directly adsorbed onto Ag(111). The structural perturbation does not lead to a significant change in the action spectrum between the monolayer and the multilayer.

5. In general, the data for a submonolayer of $Fe(CO)_5$ adsorbed on a decane spacer layer are more similar to multilayer $Fe(CO)_5$ than to a monolayer on Ag(111). This suggests interadsorbate interactions on the decane that are suppressed when the adsorbate binds to the silver surface.

6. Photochemical action spectra reveal a characteristic maximum in cross-section at 335 nm. This peak is observed independent of coverage, and whether the silver surface has been carefully annealed or extensively roughened. The latter result suggests that the peak should not be assigned to the excitation of surface plasmons (a surface-enhanced adsorbate-mediated mechanism) but should more likely be associated with a perturbation of the $Fe(CO)_5$ electronic spectrum on adsorption.

7. The photochemical yield of CO increases with increasing coverage, in contrast to the decreasing cross-section measured by PID. This is assigned partly to a greater density of photoactive sites in the multilayer compared to the monolayer. However, this cannot completely account for the increased yield. It was suggested that dark reactions between the primary photoproduct and adsorbed $Fe(CO)_5$ acts as a secondary source of (thermalized) CO.

8. A simple kinetic model has been proposed that accounts for most of these observations. For monolayer $Fe(CO)_5$, photodissociation proceeds largely through the direct photolysis mechanism. In multilayers, photodissociation proceeds with a reduced cross-section, and the photoproduct reacts with the reactant to yield a secondary product and a second thermalized CO molecule. The scheme was solved numerically and was shown to approximately reproduce the observed PID.

9. In all cases cross-section measurements have been made as a function of surface roughness. The surface was modified between carefully annealed Ag(111) and a surface roughened by extensive bombardment with energetic ions. There was no evidence for a large enhancement of the photochemical cross-section due to resonance with the surface plasmon. When the data were normalized to remove the first layer enhancement effect, there appeared to be a small enhancement of the cross-section on the roughened surface, but the effect was smaller than a factor of 2. Possibly the observation of plasmon-enhanced

adsorbate-mediated photochemistry will require a surface engineered to yield a high coverage of nanometer scale features.

Acknowledgment. We are grateful to the EPSRC for financial support, and D.J.B. thanks the EPSRC for a project studentship.

References and Notes

(1) Celii, F. G.; Whitmore, P. M.; Janda, K. C. *J. Phys. Chem.* **1988**, *92*, 1604.
(2) Lichtman, D.; Shapiro, Y. *CRC Crit. Rev. Solid State Matter* **1978**, *8*, 93.
(3) Avouris, P.; Walkup, R. E. *Annu. Rev. Phys. Chem.* **1989**, *40*, 173.
(4) *Laser Microfabrication*; Ehrlich, D. J., Tsao, J. Y., Eds.; Academic Press: New York, 1989.
(5) Ho, W. *Res. Chem. Intermed.* **1992**, *17*, 27.
(6) Guo, H.; Saalfrank, P.; Seideman, T. *Prog. Surf. Sci.* **1999**, *62*, 239.
(7) Ho, W. Surface Photochemistry. In *Laser Spectroscopy and Photochemistry on Metal Surfaces*; Dai, H.-L., Ho, W., Eds.; World Scientific: Singapore, 1995; p 1047.
(8) Hasselbrink, E. *Appl. Surf. Sci.* **1994**, *80*, 34.
(9) Hasselbrink, E. *Appl. Phys. A-Mater. Sci. Process.* **1991**, *53*, 403.
(10) Hasselbrink, E. *Ber. Bunsen-Ges. Phys. Chem. Chem. Phys.* **1993**, *97*, 1692.
(11) Zhou, X. L.; Zhu, X. Y.; White, J. M. *Surf. Sci. Rep.* **1991**, *13*, 73.
(12) Myli, K. B.; Coon, S. R.; Grassian, V. H. *J. Phys. Chem.* **1995**, *99*, 16407.
(13) Myli, K. B.; Grassian, V. H. *J. Phys. Chem.* **1994**, *98*, 6237.
(14) Goncher, G. M.; Parsons, C. A.; Harris, C. B. *J. Phys. Chem.* **1984**, *88*, 4200.
(15) Kidd, R. T.; Lennon, D.; Meech, S. R. *J. Chem. Phys.* **2000**, *113*, 8276.
(16) Kidd, R. T.; Meech, S. R.; Lennon, D. *Chem. Phys. Lett.* **1996**, *262*, 142.
(17) Wolf, M.; Zhu, X. Y.; White, J. M. *J. Chem. Phys.* **1992**, *97*, 7015.
(18) Nitzan, A.; Brus, L. E. *J. Chem. Phys.* **1981**, *75*, 2205.
(19) Gersten, J. I.; Nitzan, A. *Surf. Sci.* **1985**, *158*, 165.
(20) Sato, S.; Tanaka, S. *Appl. Surf. Sci.* **199**8, *135*, 83.
(21) Jackman, R. B.; Foord, J. S. *Surf. Sci.* **1989**, *209*, 151.
(22) Darsillo, M. S.; Gafney, H. D.; Paquette, M. S. *J. Am. Chem. Soc.* **1987**, *109*, 3275.
(23) Huang, H. H.; Sreekanth, C. S.; Seet, C. S.; Xu, G. Q.; Chan, L. *J. Phys. Chem.* **1996**, *100*, 18138.
(24) Gluck, N. S.; Ying, Z.; Bartosch, C. E.; Ho, W. *J. Chem. Phys.* **1987**, *86*, 4957.
(25) Ohmori, T.; Sato, S. *J. Photochem. Photobiol. A—Chem.* **1992**, *64*, 201.
(26) Sato, S.; Ohmori, T. *J. Phys. Chem.* **1991**, *95*, 7778.
(27) Ukisu, Y.; Sato, S.; Ohmori, T. *Appl. Organomet. Chem.* **1991**, *5*, 243.
(28) Sato, S.; Ohmori, T. *J. Chem. Soc., Chem. Commun.* **1990**, 1032.
(29) Rocklein, M. N.; Land, D. P. *Surf. Sci.* **1999**, *436*, L702.
(30) Henderson, M. A.; Ramsier, R. D.; Yates, J. T. *Surf. Sci.* **1992**, *275*, 297.
(31) Ramsier, R. D.; Yates, J. T. *J. Vac. Sci. Technol. A—Vac. Surf. Films* **1993**, *11*, 1936.
(32) Sato, S.; Ukisu, Y.; Ogawa, H.; Takasu, Y. *J. Chem. Soc.—Faraday Trans.* **1993**, *89*, 4387.
(33) Sato, S.; Suzuki, T. *J. Phys. Chem.* **1996**, *100*, 14769.
(34) Sun, L.; McCash, E. M. *Surf. Sci.* **1999**, *422*, 77.
(35) Sato, S.; Ukisu, Y. *Surf. Sci.* **1993**, *283*, 137.
(36) Kidd, R. T.; Lennon, D.; Meech, S. R. *J. Phys. Chem. B* **1999**, *103*, 7480.
(37) Vondrak, T.; Burke, D. J.; Meech, S. R. *Chem. Phys. Lett.* **2000**, *327*, 137.
(38) Zimmermann, F. M.; Ho, W. *Surf. Sci. Rep.* **1995**, *22*, 129.
(39) Kidd, R. T. Adsorbate Photochemistry—The Effects of Surface Morphology. Ph.D. Thesis, University of East Anglia, 1998.
(40) Hinsberg, W. D.; Houle, F. A. IBM Chemical Kinetics Simulator; 1.01 ed.
(41) Chien, J. *J. Am. Chem. Soc.* **1948**, *70*, 2256.
(42) Sato, S.; Ukisu, Y.; Ogawa, H.; Takasu, Y. *Appl. Surf. Sci.* **1994**, *80*, 428.
(43) Bourdon, E. B. D.; Cho, C. C.; Das, P.; Polanyi, J. C.; Stanners, C. D.; Xu, G. Q. *J. Chem. Phys.* **1991**, *95*, 1361.
(44) Zhu, X. Y. *Surf. Sci.* **1997**, *390*, 224.
(45) Giorgi, J. B.; Naumkin, F. Y.; Polanyi, J. C.; Raspopov, S. A.; Sze, N. S. K. *J. Chem. Phys.* **2000**, *112*, 9569.
(46) Buntin, S. A.; Cavanagh, R. R.; Richter, L. J. *J. Chem. Phys.* **1993**, *98*, 7651.
(47) Leadbeater, N. *Coord. Chem. Rev.* **1999**, *188*, 35.
(48) So, S. K.; Ho, W. *J. Chem. Phys.* **1991**, *95*, 656.
(49) Grevels, F. W.; Klotzbucher, W. E. *Inorg. Chem.* **1981**, *20*, 3002.
(50) Nathanson, G.; Gitlin, B.; Rosan, A. M.; Yardley, J. T. *J. Chem. Phys.* **1981**, *74*, 361.
(51) Das, P.; Metiu, H. *J. Phys. Chem.* **1985**, *89*, 4680.
(52) Sato, S.; Suzuki, T. *J. Electron Spectrosc. Relat. Phenom.* **1997**, *83*, 85.
(53) Frost, A. A.; Pearson, R. G. *Kinetics and Mechanism*; John Wiley: New York, 1961.